DR. PAUL R. WOLF*
University of California
Berkeley, Calif. 94720

DR. DONALD R. GRAFF
ITEK Corporation
Alexandria, Va. 22314

Lunar Control from Ranger Photos

Accuracy, however, cannot approach earth standards because of the inherently weak geometry of the system.

(*Abstract on page 1033*)

INTRODUCTION

ON JULY 28, 1964 RANGER VII was launched from Cape Kennedy. Its mission was to transmit to earth close-up pictures of the lunar surface. The mission was a spectacular success as more than 4,300 photographs were received. During the ensuing eight months Rangers VIII and IX were also successful in their missions bringing the total number of received close-up lunar photographs to over 17,000. This study deals with the location of points on the surface of the moon using methods of analytical photogrammetry in conjunction with Ranger photography. It is the result of research undertaken by the authors while they were on the staff of the Civil Engineering Department at the University of Wisconsin.

The authors are grateful to the Jet Propulsion Laboratory of Pasadena, California, for furnishing the necessary film strips and parameter listings for the Ranger missions which were used in this study.

* Presented at the Semi-Annual Convention of the American Society of Photogrammetry, St. Louis, Mo., October 1967, under the title, "Lunar Control Coordinates from Ranger Photography."

THEORETICAL CONSIDERATIONS

FLIGHT PARAMETERS

As successive photos in the Ranger missions contained some common area, it is pos-

DR. PAUL R. WOLF

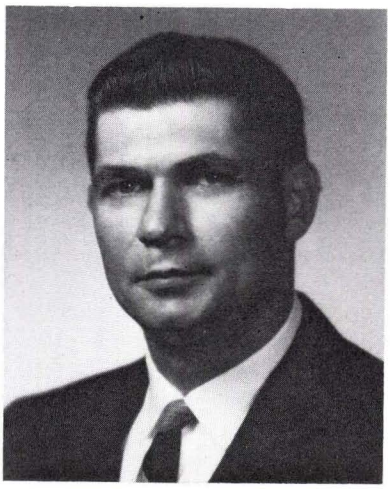

DR. DONALD R. GRAFF

sible to solve for the space position of points from measurements on the photos. This assumes that control information is available to determine the orientation and position of the exposures. The control used in this study was taken as the flight parameters determined by the Jet Propulsion Laboratory. The particular flight parameters used in this study are as follows:

1. LAT_S—The selenocentric latitude of the sub-spacecraft point. The sub-spacecraft point is the point on the lunar surface vertically beneath the spacecraft at the instant of exposure. (Degrees, Figure 1).
2. Lon_S—The selenocentric longitude of the sub-spacecraft point. (Degrees, Figure 1).
3. Lat_P—The selenocentric latitude of the point of intersection of the camera optical axis with the lunar surface. This point is herein referred to as the lunar principal point. (Degrees, Figure 1).
4. Lon_P—The selenocentric longitude of the lunar principal point. (Degrees, Figure 1).
5. *R*—The length of the vector from the lunar center to the camera at the instant of exposure. (Meters, Figure 1).
6. *Range*—The distance along the camera axis from the camera to the lunar principal point. (Meters, Figure 1).
7. *Alt*—The distance from the camera to the sub-spacecraft point. (Meters, Figure 1).
8. *AZN*—The clockwise angle measured in the plane of the photograph from the positive *y* photographic axis to lunar north. (Degrees, Figure 2).
9. *AZS/C*—The counterclockwise angle measured in the plane of the photograph from the positive *y* photographic axis to the downward or nadir end of the principal line. (Degrees, Figure 2).

ABSTRACT: *An analytical photogrammetric procedure is used for computing lunar control coordinates from Ranger photography. Flight parameters obtained from the Jet Propulsion Laboratory are used to determine the position and orientation of the photographs. Collinearity equations are used and the computations are performed in a selenocentric object space coordinate system. The procedures have been programmed for electronic computer solutions and have been tested using various combinations of overlapping photographs. Based on the test results, samples of which are tabulated herein, it is evident that probe-type photography such as Ranger can successfully be used to obtain topographic information, and similar procedures could be utilized again in future preliminary explorations of more-distant heavenly bodies.*

Computations were performed with respect to a selenocentric object space coordinate system. This proved ideal for computing coordinates from the comparatively high-altitude Ranger photos of the lunar surface whose curvature is much greater than that of the

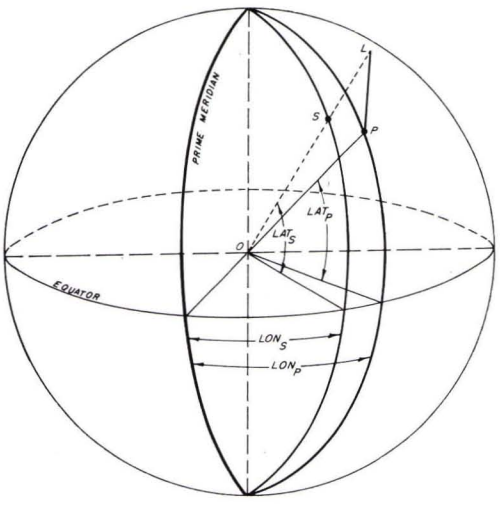

FIG. 1 Ranger flight parameters: *L*, exposure station; *S*, subspacecraft point; *P*, lunar principal point; *O*, lunar center; *LS*, altitude; *LP*, range; *LO*, *R*; *SO*, radius.

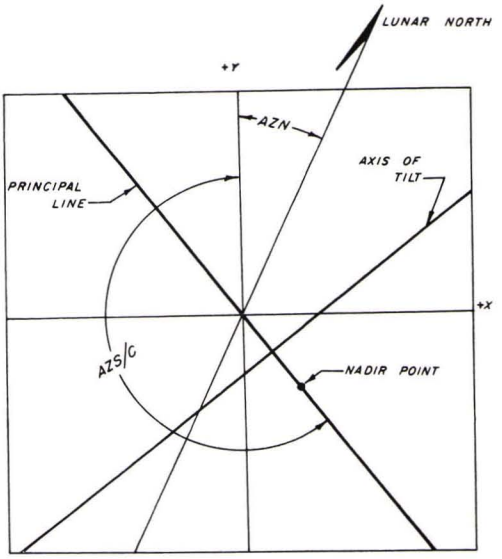

FIG. 2 Ranger photograph parameters.

earth. In the selenocentric system, the X',Y'-plane is the lunar equatorial plane, with X'-positive in the direction of the lunar prime meridian, and Z'-positive in the direction of the lunar north pole. The image space x,y-plane is defined in the plane of the photograph with the x,y-axis defined by a reseau grid and z considered positive toward the camera lens, (see Figure 3).

COORDINATE TRANSFORMATION

The image space coordinates were transformed into an *erect* coordinate system, parallel to the object space coordinate system, with a rotation matrix derived as follows:

1. Rotate x,y,z-coordinates in the plane of the photographs into x',y',z' where y' is positive in the direction of lunar north. In matrix notation:

$$\begin{bmatrix} x' \\ y' \\ z' \end{bmatrix} = \begin{bmatrix} \cos AZN & -\sin AZN & 0 \\ \sin AZN & \cos AZN & 0 \\ 0 & 0 & 1 \end{bmatrix} \begin{bmatrix} x \\ y \\ z \end{bmatrix}.$$

2. Translate x',y' and z'-coordinates to x'', y'' and z'', which places the origin at the photographic nadir point. In matrix notation:

$$\begin{bmatrix} x'' \\ y'' \\ z'' \end{bmatrix} = \begin{bmatrix} 1 & 0 & (-\tan t \cos \omega) \\ 0 & 1 & (\tan t \sin \omega) \\ 0 & 0 & 1 \end{bmatrix} \begin{bmatrix} x' \\ y' \\ z' \end{bmatrix}$$

where

$$t = \cos^{-1}\left[\frac{R^2 + (\text{Range})^2 - (\text{Radius})^2}{2 \times R \times \text{Range}}\right]$$

$$\omega = 270^\circ - AZS/C - AZN.$$

3. Transform x'', y'' and z''-coordinates to x''', y''', and z''' which lie in a plane perpendicular to the local normal to the lunar surface. In matrix notation:

$$\begin{bmatrix} x''' \\ y''' \\ z''' \end{bmatrix} = \begin{bmatrix} \cos \phi & 0 & 0 \\ 0 & \cos \theta & 0 \\ \sin \phi & -\sin \theta & \text{Sec } t \end{bmatrix} \begin{bmatrix} x'' \\ y'' \\ z'' \end{bmatrix}$$

where

$$\theta = \sin^{-1}(\sin \omega \sin t)$$

$$\varphi = \sin^{-1}(\cos \omega \sin t).$$

4. Transform x''', y''', and z'''-coordinates to x^{iv}, y^{iv} and z^{iv} which are in a plane parallel to the object space X', Y'- plane.In matrix notation:

$$\begin{bmatrix} x^{iv} \\ y^{iv} \\ z^{iv} \end{bmatrix} = \begin{bmatrix} 1 & 0 & 0 \\ 0 & \text{Cos } \psi & \text{Sin } \psi \\ 0 & -\text{Sin } \psi & \text{Cos } \psi \end{bmatrix} \begin{bmatrix} x''' \\ y''' \\ z''' \end{bmatrix}$$

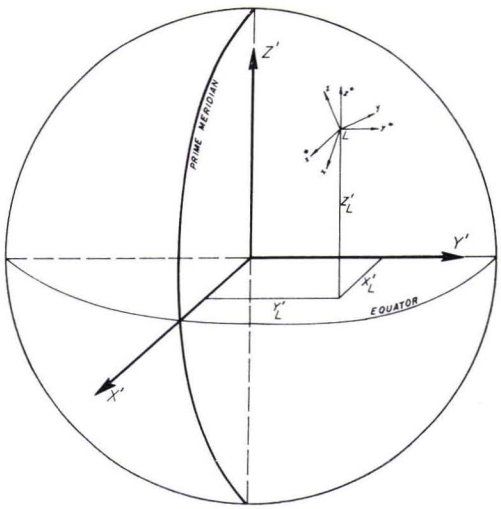

FIG. 3 Image and object space coordinate systems.

where

$$\psi = 90^\circ - \text{Lat}_S.$$

5. Rotate x^{iv}, y^{iv} and z^{iv} into the erect x^*, y^*, z^*-system such that $+x^*$ is in the direction of $+X'$ as shown in Figure 3. In matrix notation:

$$\begin{bmatrix} x^* \\ y^* \\ z^* \end{bmatrix} = \begin{bmatrix} \cos \beta & -\sin \beta & 0 \\ \sin \beta & \cos \beta & 0 \\ 0 & 0 & 1 \end{bmatrix} \begin{bmatrix} x^{iv} \\ y^{iv} \\ z^{iv} \end{bmatrix}$$

where

$$\beta = 90^\circ + \text{Lon}_S.$$

The final rotation matrix M, which is used to determine x^*, y^*, z^*-coordinates from the measured image coordinates x,y and the focal length z, is the product of the individual matrices such that:

$$\begin{bmatrix} x^* \\ y^* \\ z^* \end{bmatrix} = \begin{bmatrix} m_{11} & m_{21} & m_{31} \\ m_{12} & m_{22} & m_{32} \\ m_{13} & m_{23} & m_{33} \end{bmatrix} \begin{bmatrix} x \\ y \\ z \end{bmatrix}$$

CONDITION EQUATIONS

The collinearity condition equations as stated in the *Manual of Photogrammetry* were utilized in computing the object space coordinates of the lunar points. A Taylor series substitution was used to linearize the equations and first approximations were obtained from the following explicit equations which are derived from Figure 4:

$$(1)\ Z_P' = [(X_{L2}' - X_{L_1}')z_1^* z_2^* - Z_{L_1}' x_1^* z_2^* + Z_{L2}' x_2^* z_1^*] \div (x_2^* z_1^* - x_1^* z_2^*)$$

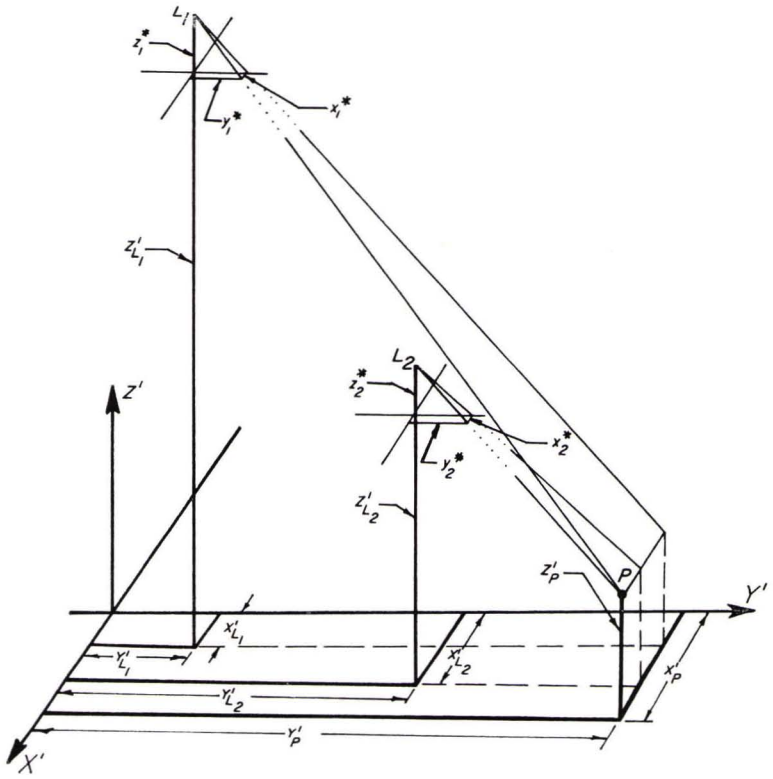

FIG. 4 Collinearity geometry.

$$X_P' = x_1^*(Z_{L_1}' - Z_P')/z_1^* + X_{L_1}' \tag{2}$$

$$Y_P' = y_1^*(Z_{L_1}' - Z_P')/z_1^* + Y_{L_1}' \tag{3}$$

The redunancy in the condition equations (four or more equations and three unknowns for each unknown point) allowed a least squares solution whereby photo coordinate residuals were minimized in the computation of the object space coordinates. After the adjusted object space coordinates of a point were determined, these were converted to latitude, longitude and elevation with respect to the lunar sphere.

APPLICATION OF THE THEORY

Photographs from all three Ranger missions were used successfully to test the foregoing analytical photogrammetric theory; however, Ranger IX photos were used most extensively.

THE PHOTOGRAMMETRIC QUALITY OF THE RANGER PHOTOGRAPHY

It must be realized at the outset that the standards of accuracy obtainable with Ranger photogrammetry can not approach the standards of accuracy obtainable with conventional earth photogrammetry. Some of the primary factors which contribute to this are: (1) the extremely small scales of the photographs; (2) the absence of a precise basic lunar control network; (3) sub-standard cameras and camera calibration data; (4) the difficulty in marking corresponding points which is caused not only by the non-existence of discrete points on the lunar surface, but also by the drastic scale changes from one photograph to the next; and (5) the extremely weak geometric quality of the Ranger photography.

The weak geometric quality of the Ranger photography, which is evaluated by the base-height B/H ratio, is due to the high angle of inclination of the spacecraft trajectory, as shown on Figure 5. The B/H ratios for three of the lowest altitude Ranger IX B-camera pairs of photographs are listed in Table I. The equation shown on Figure 5, was used to calculate the B/H ratios for this unconventional Ranger photography.

It is noted from Table I that an increase in

the B/H ratio may be realized by using non-adjacent photographs rather than adjacent photos. This increase in the B/H ratio, however, is accompanied by a corresponding decrease in resolution as a consequence of taking higher-altitude, smaller-scale photographs to complete the pairs.

In a recent instrumental photogrammetric study[5] it was found, as would be expected, that photogrammetric accuracy decreases with a corresponding decrease in the B/H ratio. In fact, it was reported that average standard deviations in Z increased by a factor of approximately 7 for a B/H ratio of 0.032 as compared to a conventional 0.60 B/H ratio.

In spite of the comparative weaknesses of the Ranger photographs from a photogrammetric standpoint, they were far superior to any other previous lunar photographs available, and the success of the Ranger missions represent truly monumental accomplishments by American engineers and scientists.

MENSURATION

The determination of the x and y photo coordinates of corresponding imagery was a three-stage procedure involving: (1) the identification of discrete images in the overlap areas of the photographs; (2) the measurement of the photo coordinates, and (3) the correction of the photo coordinates for image distortion.

The identification of discrete points posed a rather difficult problem with the Ranger photography for two reasons. Not only are discrete points rare on the lunar surface, but the problem was further complicated by the extreme photographic scale changes from one photograph to the next caused by the rapid descent of the spacecraft. Two approaches were taken in the point identification problem. In the first approach corresponding points were marked monoscopically. In the second approach the photographs were brought to a common scale, points were marked monoscopically on the photographs with the highest resolution, and then the corresponding points were transferred stereoscopically.

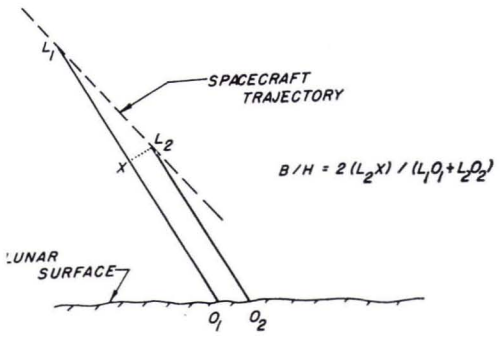

FIG. 5 Ranger B/H ratio geometry.

TABLE I. BASE-HEIGHT RATIOS FOR SELECTED RANGER IX B-CAMERA STEREO PAIRS

Frame Nos.	*B/H Ratios*
435–437	0.032
437–439	0.054
435–439	0.081

Photo coordinate observations were made with a glass scale capable of obtaining readings to the nearest 10 microns by estimation. The Ranger A-camera and B-camera photographs contained a calibrated 25-point reseau grid. Observations made on the grid marks indicated that substantial image distortions were present, as shown by the variation in observed distances between adjacent reseau marks for Ranger IX photo No. 439 illustrated on Figure 6.

The observed photo coordinates were corrected for image distortions by applying a projective transformation. Using this method each of the 16 small squares bounded by a set of four grid marks was treated as a separate unit.

SAMPLE RESULTS OF LUNAR CONTROL COORDINATE COMPUTATION

The previously cited Ranger analytical

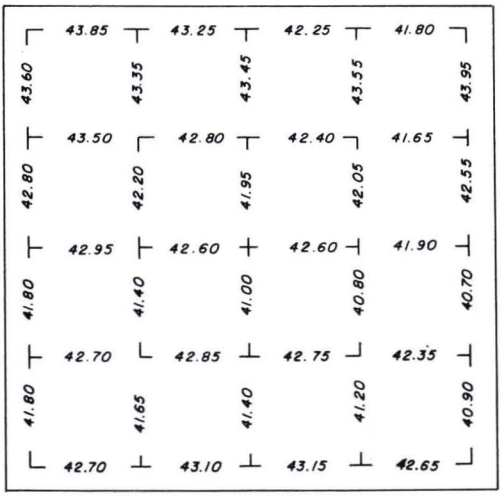

FIG. 6 Observed distances (mm) Ranger IX B-camera #439 Reseau.

TABLE II. LUNAR CONTROL COORDINATES FROM RANGER IX PHOTOS
(Monoscopic Print Transfer)

Point	B-Camera Photos 435-437-439						B-Camera Photos 435-439					
	Selenocentric Coordinates (meters)			South Latitude, West Longitude and Elevation (meters)			Selenocentric Coordinates (meters)			South Latitude, West Longitude and Elevation (meters)		
	X'	Y'	Z'	Lat	Long	h	X'	Y'	Z'	Lat	Long	h
1	1,692,484	68,318	384,381	12.785	2.312	328	1,692,450	68,292	384,374	12.785	2.311	292
2	1,692,416	68,938	384,641	12.794	2.333	343	1,692,344	68,890	384,624	12.794	2.331	268
3	1,692,434	69,135	384,654	12.794	2.339	372	1,692,366	69,088	384,638	12.794	2.338	300
4	1,692,410	68,947	384,784	12.799	2.333	370	1,692,333	68,896	384,765	12.799	2.331	289
5	1,692,420	69,269	385,050	12.807	2.344	452	1,692,348	69,224	385,034	12.807	2.342	376
6	1,692,405	68,135	385,061	12.808	2.305	394	1,692,344	68,092	385,047	12.808	2.304	331
7	1,692,231	67,785	385,401	12.820	2.294	286	1,692,185	67,751	385,392	12.820	2.293	238
8	1,692,237	67,866	385,374	12.819	2.297	289	1,692,209	67,846	385,370	12.819	2.296	261
9	1,692,150	67,317	385,745	12.832	2.278	266	1,692,102	67,281	385,736	12.832	2.277	216
10	1,692,171	68,657	386,316	12.850	2.323	466	1,692,093	68,606	386,304	12.850	2.322	385

photogrammetric procedures were programmed in Fortran and executed on an electronic computer. The program would accept a stereo pair or several photographs in a strip and perform a simultaneous least squares adjustment of all rays intersecting at a point. Equal weights were assumed for all measured photo coordinates.

The program output included the object space selenocentric X', Y', and Z'-coordinates of each point together with estimations of the standard deviations in these coordinates. The output also included the latitude, longitude, and elevation for each point. The latitudes and longitudes were obtained to the nearest 0.001 degrees, which corresponds to a distance of 30 meters on the lunar surface.

Various computer runs were made utilizing different combinations of stereo pairs, triplets, and quadruplets, and incorporating the photo coordinates obtained by both the monoscopic and stereoscopic point marking procedures. Sample results for four runs are presented in Tables II and III. Table II contains the results of a triplet solution and a stereo pair solution utilizing only monoscopically marked points. Table III lists the results obtained from the same triplet and stereo pair but using stereoscopically marked points. The points reported in Table II do not correspond to the points reported in Table III.

Table IV lists the average estimated standard deviations of unit weight in the measured photo coordinates, S_o, and the average estimated standard deviations in the computed selenocentric coordinates, $S_{X'}$,$S_{Y'}$ and $S_{Z'}$, for the four runs which are reported in Tables II and III.

It may be noted from Table IV that the average estimated standard deviations in the selenocentric coordinates are improved in the triplet solutions as opposed to the stereo pairs. This observation suggests that even more improvement may be obtained by including more than three photos in the simul-

TABLE III. LUNAR CONTROL COORDINATES FROM RANGER IX PHOTOS
(Stereoscopic Point Transfer)

Point	B-Camera Photos 435-437-439						B-Camera Photos 435-439					
	Selenocentric Coordinates (meters)			South Latitude, West Longitude and Elevation (meters)			Selenocentric Coordinates (meters)			South Latitude, West Longitude and Elevation (meters)		
	X'	Y'	Z'	Lat	Long	h	X'	Y'	Z'	Lat	Long	h
1	1,692,409	68,251	384,371	12.786	2.309	250	1,692,390	68,234	384,365	12.786	2.309	229
2	1,692,398	68,915	384,637	12.794	2,332	324	1,692,389	68,906	384,636	12.794	2,332	315
3	1,692,389	69,234	385,040	12.807	2.343	418	1,692,359	69,212	385,034	12.807	2.342	387
4	1,692,593	68,222	385,092	12.807	2.308	588	1,692,556	68,196	385,080	12.807	2.307	548
5	1,692,493	68,972	385,249	12.813	2.334	554	1,692,481	68,962	385,249	12.813	2.333	542
6	1,692,238	67,821	385,395	12.820	2.295	293	1,692,221	67,809	385,389	12.820	2.295	275
7	1,692,407	68,543	385,734	12.829	2.319	562	1,692,383	68,526	385,727	12.829	2.319	536
8	1,692,126	67,283	385,749	12.832	2.277	242	1,692,108	67,268	385,744	12.832	2.277	223
9	1,692,090	68,610	386,309	12.850	2.322	383	1,692,048	68,580	386,299	12.850	2.321	338

TABLE IV. SUMMARY OF AVERAGE ESTIMATED STANDARD DEVIATIONS IN THE MEASURED PHOTO COORDINATES AND IN THE COMPUTED SELENOCENTRIC COORDINATES

Combination of Photographs Used	*Monoscopic Point Transfer*				*Stereoscopic Point Transfer*			
	So (*mm*)	*SX'* (*meters*)	*SY'* (*meters*)	*SZ'* (*meters*)	*So* (*mm*)	*SX'* (*meters*)	*SY'* (*meters*)	*SZ'* (*meters*)
435–437–439	±0.330	±94	±59	±21	±0.296	±99	±60	±20
435–439	±0.478	±178	±114	±43	±0.431	±154	±93	±33

taneous solution. That procedure is often precluded, however, by the disappearance of corresponding imagery in the additional higher altitude photographs as a consequence of the scale change factor. A second observation made from Table IV is the decreased magnitudes of the estimated standard deviations in the measured x and y photo coordinates with the point transfer being accomplished stereoscopically. This would suggest that stereoscopic point transfer is superior to monoscopic point transfer in the Ranger photos.

SUMMARY

A method has been presented for the analytical photogrammetric determination of lunar control coordinates from Ranger photography. The method has been tested using various combinations of overlapping Ranger photographs and sample results of these tests are tabulated herein. Based on the test results it is evident that probe-type photography such as Ranger can be used to obtain topographic information and could be contemplated in future probes to more-distant heavenly bodies. The standards of accuracy of the topographic determinations can not, however, approach the standards of accuracy for conventional photography due primarily to the weak geometric quality of the photography which necessarily results from probe-type missions. From a photogrammetric standpoint, recent technological accomplishments with Lunar Orbiters have produced more desirable photographs than Rangers for extracting lunar topographic data.

REFERENCES

1. American Society of Photogrammetry, *Manual of Photogrammetry*, Third Edition, George Banta Publishing Co., Menasha, Wis., 1966.
2. Alderman, J. D., Borgeson, W. T., and Wu, S. S. C., "Investigations of the Photogrammetric Potential of the Ranger Imagery," Report from the U. S. Geological Survey, Washington, D. C., Oct. 1966.
3. Barry, R. G. and Courtney, T. P., "Selenodotic Control from Ranger Photography," PHOTOGRAMMETRIC ENGINEERING, Vol. XXXIV, No. 3, March 1968, pp. 274–282.
4. Bowles, Lawrence D., "Cartographic Experimentation with Ranger Photography," Presented at the Semi-annual Meeting of the American Society of Photogrammetry, Dayton, Ohio, September 1965.
5. Harpe, R., "Experiments with Minimum to Optimum Base-Height Ratios," Presented at the Semi-annual Meeting of the American Society of Photogrammetry, Dayton, Ohio, Sept. 1965.
6. Hedden, R. T., "Lunar Charting Experiments Using Ranger Materials in the SS-11A Analytical Plotter," Presented at the Annual Meeting of the American Society of Photogrammetry, Washington, D. C., March 1966.
7. Kirhofer, W. E., and Willingham, D. E., "Ranger VII, VIII and IX Photographic Parameters," *NASA Technical Reports* No. 32–964, 32–965 and 32–966, Jet Propulsion Laboratory, Pasadena, California, 1966.
8. Light, Donald L., "Ranger Mapping by Analytics," PHOTOGRAMMETRIC ENGINEERING, Vol. XXXII, No. 5, Sept. 1966, pp. 792–800.
9. Schurmeier, H. M., Heacock, R. L., and Wolfe, A. E., "The Ranger Missions to the Moon," *Scientific American*, Vol. 214, No. 1, 1966. pp. 52–67.